KSME

Springer

Journal of Mechanical Science and Technology 36 (12) 2022

Original Article
DOI 10.1007/s12206-022-1118-2

Keywords:
· Method of characteristics
· Supersonic flow
· Ideal contour nozzle
· Shocks

Correspondence to:
Junaid H Masoodi
junaidmasoodi@uok.edu.in

Citation:
Rafiq, K., Rasheed, M., Afzal, M. M., Masoodi, J. H. (2022). Influence of ideal nozzle geometry on supersonic flow using the method of characteristics. Journal of Mechanical Science and Technology 36 (12) (2022) 6027~6039.
http://doi.org/10.1007/s12206-022-1118-2

Received January 22nd, 2022
Revised July 7th, 2022
Accepted August 11th, 2022

† Recommended by Editor
Han Seo Ko

Influence of ideal nozzle geometry on supersonic flow using the method of characteristics

Khalid Rafiq, Mumin Rasheed, Mir Moin Afzal and Junaid H Masoodi

Department of Mechanical Engineering, Institute of Technology, University of Kashmir, Zakura Campus, Srinagar 190006, India

Abstract The present study addresses the application of the method of characteristics (MoC) for determining the thermodynamic and flow properties of the supersonic flow field in the divergent section of an ideal contour nozzle (ICN). An algorithm for developing the wall profile of the ICN using MATLAB programmable finite difference computational functions is discussed. Sixteen ICNs having different geometries are analyzed to study the influence of throat geometric parameters on the properties of the fluid in their divergent section. A sudden change in the Mach number or weak shocks is observed in asymmetric nozzles, i.e., nozzles where the radius of curvature on the convergent and divergent sides is different. Furthermore, it is observed that ICNs with an equal convergent and divergent radius of curvature are capable of developing stable supersonic flow in its divergent section.

1. Introduction

The method of characteristics (MoC) was first introduced as a general solution procedure for partial differential equations by Hadamard in 1903 and later improved by Levi-Civita in 1932 [1]. Using this method, the hyperbolic partial differential equations defining fluid flow within the divergent section of the nozzle can be reduced to a set of coupled ordinary differential equations. Prandtl [2] in 1929 first introduced this method for the development of shock-free contours in supersonic nozzles by adopting a graphical approach for the study of inviscid, irrotational, and supersonic flows. Shiparo [3] introduced an analytical approach to the two-dimensional method of characteristics. Guentert [4] designed an axis-symmetric nozzle and expressed that a practical solution can be developed by starting from an estimated pressure distribution along the axis of symmetry of the nozzle. Using this method and considering the initial expansion of the characteristic lines or Mach lines through a sharp corner at the nozzle throat, Guderley [5] developed the maximum thrust nozzle of a given length. The maximum thrust nozzle contours for given ambient pressure and length were introduced by Rao [6] using Lagrange multipliers along with the Guderley formulation. Ahlberg et al. [7] provided an alternative to Rao [6] nozzles by truncating ideal contour nozzles (nozzles that provide a parallel, uniform supersonic flow at the exit) to shorter lengths. Gogish [8] proposed a design procedure for creating extremely short nozzles by linearly compressing the TIC nozzles to develop better thrust nozzles in comparison to Rao [6] nozzles for the same envelope (i.e., same area-ratio and length).

Ideal contour nozzles or perfect nozzles consist of a throat with a circular arc at its upstream and downstream regions, followed by a turning contour developed by considering the consistency of mass flow rate throughout the nozzle. This nozzle expands the sonic flow at the throat into the supersonic flow at the exit duct with a uniform axial flow of a desired Mach number or area ratio [7].

The flow analysis in the divergent section of the ICN is initiated from a surface that is barely supersonic and is called the initial value line (IVL) that is located in the throat region, slightly downstream of the sonic line (locus of all the points within the flow field having a unit Mach

number). As a result, flow in the throat (where the transition from subsonic to supersonic flow occurs) region has been widely studied, and various expansion techniques [9-11] have been applied to study the transonic region in the throat. All these methods are based on the perturbation of one-dimensional flow through the normalized throat radius of curvature ($R_a = \rho_u / t_h$). Sauer [9] developed the earliest approximation formulas for the position and form of the sonic line in the neighborhood of the nozzle throat section using small perturbation techniques. With these techniques, axisymmetric compressible fluid flow equations are solved. The solution is proposed as an expansion series in terms of the inverse of the normalized throat radius of curvature. The method is adequate for analyzing the transonic flow field in gradual throat contours ($R_a > 2$), but diverges for small values of R_a [12].

The results generated by MoC for the supersonic flow field are a function of the nature of the gas. The gas is usually considered calorically and thermally perfect. However, for high values of stagnation pressure and stagnation temperature, the specific heat and their ratio do not remain constant and start to vary with temperature. Zebbiche et al. [13, 14] developed a mathematical model of gas at high temperature and pressure by incorporating the variation of specific heat and their ratios with elevated stagnation pressure and temperature. This model predicts that a perfect gas relation could be used to study the supersonic flow of the desired Mach number with an error less than 5 % only if the stagnation temperature is lower than 1000 K and the stagnation pressure is moderate.

Ideal contour nozzles form the base profile of high impulse nozzles such as truncated ideal contour nozzles (e.g., LR-115, RD-0120) [15] and altitude compensating nozzles such as dual bell nozzles. The dual bell nozzles are a relatively recent concept that provides promising results among various altitude compensating nozzles and are finding applications in CubeSats [16] and small, private satellites. Somewhat surprisingly, the literature available on the design of an ideal contour nozzle is extremely scant. In contrast, abundant literature is available for the design of a minimum length nozzle (nozzles having a sharp corner instead of a circular arc downstream of the throat) using MOC. The turning contour in one of the famous thrust nozzles (Rao nozzles) is also based on the consistency of the mass flow rate. However, very few details about how Rao performed the continuity calculations are available. Zucrow and Hoffman [17, 18] provide the closest implementation of the method of characteristics for the design of ICN; however, a significant gap exists between the theory provided and the implementation of this theory in the design of ICN.

The present study provides a detailed procedure for the design and analysis of an ICN for the desired Mach number and also studies the variation of thermodynamic (P, T, ρ and M and flow properties (u, v) of the fluid with changes in nozzle design parameters such as (ρ_u, ρ_d, t_h). Gas with γ = 1.4 and R = 287 J/kg-K is used throughout the analysis and is assumed to be calorically and thermally perfect. A normalized throat radius of curvature greater than or equal to 2 is employed. Sauer's method is used to analyze the transonic flow in the throat region and to develop an IVL that acts as the base surface for the implementation of MoC. The modified-Euler-predictor-corrector method [19, 20], a second-order method for integrating total differential equations resulting from the application of MoC to a supersonic flow field, is used to develop finite difference equations and is applied throughout this work. The corrector step of the iterative process is based on the average property method as Hoffman [21] showed that more accurate results are obtained by taking the average value of the thermodynamic and flow properties at the initial and solution points.

Apart from filling the literature gap on the application of MOC in designing an ICN, the paper provides a detailed study of the geometric variable influence on the stability (in terms of shock) of supersonic flow in the divergent section of the nozzle. Nozzles with an asymmetric radius of curvature on the convergent and divergent sides embody weak shocks. Symmetric nozzles (i.e., $\rho_d = \rho_u$) develop a supersonic flow with smooth thermodynamic and flow property variation (i.e., no shocks) in the divergent section of the ICN. The geometric conditions under which the shocks are developed are of high importance. These shocks may lead to asymmetric flow separation resulting in dangerous lateral forces known as side-loads [22], which can prove detrimental to nozzle assembly [23].

2. Numerical modelling

2.1 Governing equations

The gas-dynamic equation [17] for a steady, inviscid, two-dimensional planar or axis-symmetric flow in cartesian coordinates is given by:

$$\left(u^2-a^2\right)\frac{\partial u}{\partial x}+\left(v^2-a^2\right)\frac{\partial v}{\partial y}+2uv\frac{\partial u}{\partial y}-\frac{\delta a^2 v}{y}=0. \quad (1)$$

Planar and axis-symmetric fluid flow are determined by values of δ, where δ = 0 for a planar flow and δ = 1 for an axis-symmetric flow. Speed of sound $\left(a=\sqrt{rRT_0-(r-1)\left(u^2+v^2\right)/2}\right)$ for a thermally and calorically perfect gas is in algebraic form and is applicable throughout the flow-field. The irrotationality condition for the fluid element in the x-y plane is satisfied by the equation:

$$\omega_z=0 \text{ or } \partial u/\partial y=\partial v/\partial x . \quad (2)$$

2.2 Method of characteristics (MoC) [17]

Application of MoC to the coupled system of partial differential equations, i.e., gas dynamic equation (Eq. (1)) and the irrotationality condition (Eq. (2)), reduces them to non-linear total differential equations given by:

$$\left(\frac{dy}{dx}\right)_{\pm}=\lambda_{\pm}=\tan\left(\theta\pm\alpha\right), \quad (3)$$

$$\left(u^2\text{-}a^2\right)du_{\pm}+\left[2uv\text{-}\left(u^2\text{-}a^2\right)\lambda_{\pm}\right]dv_{\pm}\text{-}\left(\frac{\delta a^2 v}{y}\right)dx_{\pm}=0\,. \tag{4}$$

The complete geometry of characteristic lines is described by Eq. (3) and is called the characteristic equation (subscripts '+' and '-' represent the left running and right running characteristics, respectively, in the x-y plane), while Eq. (4) is called the compatibility equation and it represents the variation of '*u*' and '*v*' for each characteristic line described by the characteristic equation. The modified-Euler-predictor-corrector [19, 20] method is applied to Eqs. (3) and (4) and the resulting finite difference equations obtained are:

$$\Delta y_{\pm}=\lambda_{\pm}\Delta x_{\pm} \tag{5}$$

where $\lambda_{\pm}=\tan\left(\theta\pm\alpha\right)$

$$Q_{\pm}\Delta u_{\pm}+R_{\pm}\Delta v_{\pm}\text{-}S_{\pm}\Delta x_{\pm}=0 \tag{6}$$

where $Q=U^2\text{-}a^2$, $R=2uv\text{-}\left(u^2\text{-}a^2\right)\lambda$ and $S=\delta a^2 v/y$.

2.3 Unit processes (solvers)

The finite difference equations provided above are used to form computational functions called the unit processes. Three different unit processes [17] or solvers, namely, 'internal point solver (IPS)', 'symmetry point solver (SPS)', and the 'inverse interior point solver (IIPS)' are programmed in MATLAB to generate the profile of ICN and study the variation of thermodynamic and flow properties inside this profile by discretizing the problem domain. A brief description of these solvers is provided below:

a) Interior point solver (IPS) It defines the geometric and flow properties of an unknown node generated by the intersection of left and right running characteristics originating from two known nodes in the flow field. The initial location of the unknown node is estimated by the intersection of two straight characteristics of opposite families (i.e., a Goursat problem) and is known as the predictor step. Suppose flow and thermodynamic properties at 'node 1' (on RRC, Fig. 1) and 'node 2' (on LRC, Fig. 1) are known, and the location of 'node 3' (formed by the intersection of RRC and LRC from node 1 and 2, respectively) is obtained by:

$$\begin{bmatrix}\text{-}\lambda_{+} & 1\\ \text{-}\lambda_{\text{-}} & 1\end{bmatrix}\begin{bmatrix}x_3\\ y_3\end{bmatrix}=\begin{bmatrix}y_2\text{-}\lambda_{+}x_2\\ y_1\text{-}\lambda_{\text{-}}x_1\end{bmatrix} \tag{7}$$

where (x_1, y_1), (x_2, y_2) represent the coordinates of known nodes, and (x_3, y_3) represent the coordinates of the unknown node. The velocity components (u_3, v_3) at 'node 3' are given by:

$$\begin{bmatrix}Q_{+} & R_{+}\\ Q_{\text{-}} & R_{\text{-}}\end{bmatrix}\begin{bmatrix}u_3\\ v_3\end{bmatrix}=\begin{bmatrix}S_{+}\left(x_3\text{-}x_2\right)+Q_{+}u_2+R_{+}v_2\\ S_{\text{-}}\left(x_3\text{-}x_1\right)+Q_{\text{-}}u_1+R_{\text{-}}v_1\end{bmatrix}. \tag{8}$$

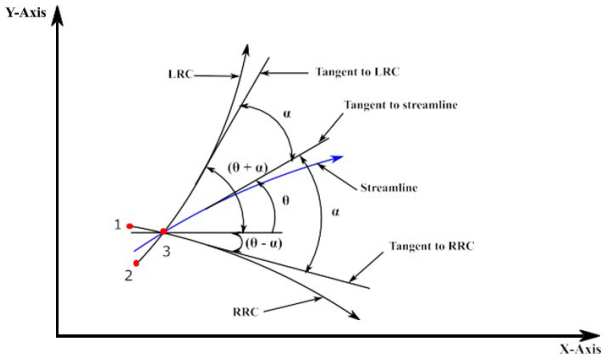

Fig. 1. Illustration of left and right running characteristic.

Once the location and velocity of the unknown node are determined, it is possible to calculate the Mach number and static thermodynamic properties (pressure, temperature, density) using the basic isentropic compressible flow relations [24].

In the predictor step, values of flow properties at node 2 ($x_+, y_+, u_+ \text{ and } v_+$) and node 1 ($x_-, y_-, u_- \text{ and } v_-$) are used in linear Eqs. (7) and (8) to provide the first estimation of the location and velocity at the unknown node 3 (x_3^0, y_3^0, u_3^0, v_3^0). The predictor step is followed by a corrector step where the flow properties at known nodes (1 and 2) are replaced by average values of flow properties between the known nodes and the unknown node (determined from the predictor step). These average values are again used in Eqs. (7) and (8) to update the solution at node 3(x_3^1, y_3^1, u_3^1, v_3^1). This terminates a single iteration of the corrector step based on the average property method. This corrector step can be iterated a number of times until a minimum acceptable error is achieved. The present study uses two iterations of the corrector.

b) Symmetry point solver (SPS) A symmetry point solver is a special case of an IPS where the two known nodes lie on the opposite sides of the nozzle axis, with the axis acting as symmetry. The abscissa and axial velocity components of two known nodes are the same, while the ordinate and radial velocity components have the same magnitude but opposite signs [17]. On the axis-symmetry node, the values of ordinate, radial velocity, and the angle between flow direction and nozzle axis are all zero.

c) Inverse interior point solver (IIPS) For flows with high property gradients, it is better to prespecify the coordinates of the nodes to control the geometric spacing between the nodes and then apply MoC to determine the flow properties (u and v) at these prespecified nodes [17].

The location of the nodes on the circular arc is pre-defined by design parameters ρ_d and $\Delta\theta_c$. The unknown flow properties (u and v) of the node lying on the circular arc extension (i.e., unknown node) are calculated by using IIPS from two known nodes lying on the previous RRC in the flow field [17]. An LRC line is projected rearwards from the prespecified wall point to intersect the previous RRC line, and the coordinates of this point (known as an inverse interior point) determine the nodes lying on this RRC that are to be used in IIPS to determine the

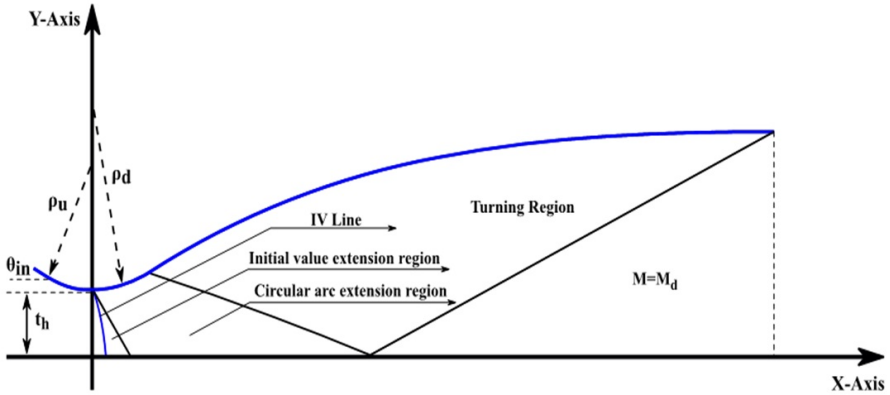

Fig. 2. Schematic of an Ideal contour nozzle.

flow properties of the unknown node. The criterion for selecting these two nodes on this RRC is that they should bracket the inverse interior point [25]. The flow properties of the inverse interior point are taken as the average flow properties of the nodes bracketing it. Modified-Euler's-predictor-corrector method up to two stages of the corrector is used to provide better results for the properties of inverse interior points which in turn affects the flow properties of the unknown node.

These unit processes or solvers were developed as subroutines. They were then integrated to form a master logic MATLAB program capable of constructing the ICN and solving the supersonic flow field inside it.

2.4 Application of unit processes (solvers) for constructing a divergent section of ICN

An ideal contour nozzle consists of three main subparts:

i) Initial value line and its extension;

ii) Circular arc extension (or Kernel region);

iii) Turning region.

i) Initial value line and its extension The supersonic IVL is the locus of the nodes for which 'v = 0', and is located downstream of the sonic line. Along this line, the Mach number is barely supersonic and is used to initiate the computation in the divergent section of the ICN. The throat height (t_h) is discretized by a user-defined number of nodes, and these nodes are used in the IVL equation [9] given below to generate the parabolic IVL contour.

$$x=\frac{-(\gamma+1)\zeta y^2}{2(3+\delta)}. \tag{9}$$

$\zeta = \sqrt{(1+\delta)/(\gamma+1)\rho_u y_t}$ is a constant (termed as the coefficient of linear non-dimensional axial perturbation velocity).

The initial value line is succeeded by its extension, which determines the thermodynamic and flow properties of the fluid downstream of the IVL with the help of the unit processes (solvers).

The extension begins by using IPS on any two successive nodes on the IVL, either starting from the wall node or the axis

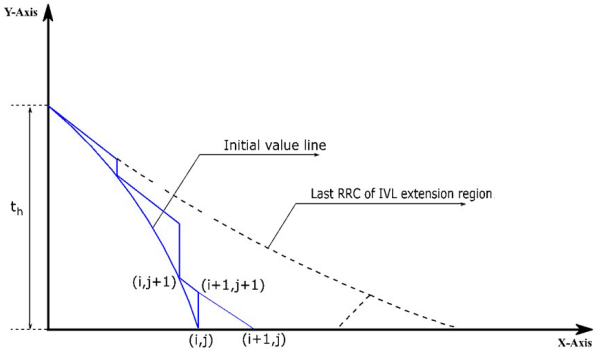

Fig. 3. Schematic of the IVL and mesh generation in the extension region.

of symmetry node. The present computation started from the axis-symmetry node represented by (i, j) in Fig. 3.

The location of the nodes on IVL and the flow velocities corresponding to these nodes formed the input parameters for the IPS. The location and properties of the unknown nodes were then determined by the IPS, and as such, it formed an important function for developing the mesh.

$$g(i+1, j+1)=\mathrm{IPS}[g(i,j), g(i, j+1)] \tag{10}$$

where '*g*' represents the thermodynamic and flow properties of the fluid as a function of the location.

Connecting the set of these nodes forms an incomplete RRC, which is terminated by connecting it to the axis of symmetry by using the SPS, i.e.,

$$g(i+1, j) = \mathrm{SPS}\left[g(i+1, j+1)\right]. \tag{11}$$

This completes the first RRC extending from the IVL. This procedure is repeated until all the nodes on the IVL generate RRC that terminates at the nozzle axis. For '*n*' nodes taken on IVL, a total of n^2 nodes are obtained on the IVL and its extension.

ii) Circular arc extension The flow field from the circular arc is generated by defining the location of nodes by using input design parameters, such as ρ_d and $\Delta\theta_c$. The flow

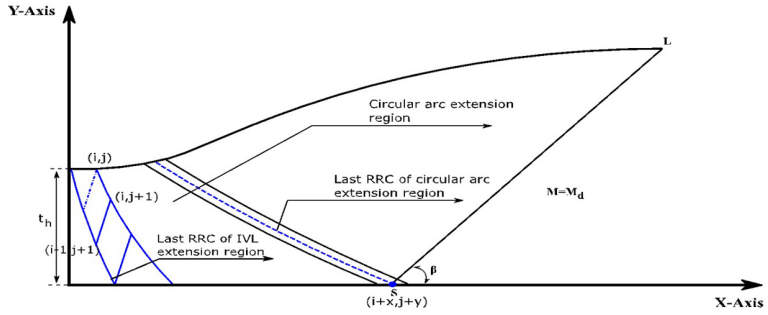

Fig. 4. Schematic of mesh generation in circular arc extension region.

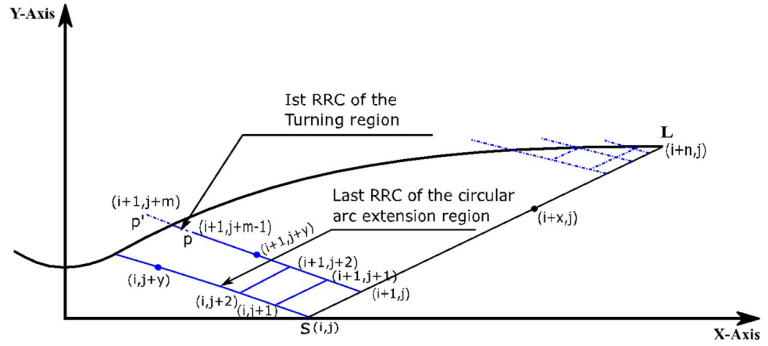

Fig. 5. Schematic of mesh generation in the turning region.

properties of the first predefined node on the downstream side of the throat circular arc are obtained by using IIPS. An interior-point solver (IPS) is used to generate the node of an RRC extending from the circular arc by using the circular arc node and lower node of the last RRC extending from IVL that satisfies the bracketing criterion.

$$g(i,j+1)=\mathrm{IPS}[g(i-1,j+1),g(i,j)]. \tag{12}$$

Successive IPS are used between the nodes on the RRC extending from the circular arc node and the corresponding nodes lying on the last RRC extending from IVL. This RRC is terminated at the axis of symmetry by using SPS, and the Mach number at this node is thus evaluated.

The entire procedure is repeated for each node on the circular arc until the Mach number at the axis of symmetry is greater than desired Mach number (M_d). Interpolation of the flow properties between the axis symmetry node on the last RRC and the corresponding node on the previous RRC is performed to find a point on the axis (represented as point 'S') with the desired Mach number. No further increase in Mach number is required, and all the characteristics beyond this node must be straight lines with an angle $\beta=(1/M_d)$.

The length of this final LRC is limited by using the mass flow rate consistency, where the mass flow rate across SL is equal to the flow rate through the IVL. The length of SL is determined as:

$$|SL|=\sqrt{\frac{\dot{m}_{num}}{\pi\rho(i+x,j+y)u(i+x,j+y)}}. \tag{13}$$

Along and beyond this characteristic, the flow and the thermodynamic properties of the fluid are constant, and a uniform axial flow with desired Mach number is achieved.

iii) Turning section This section contributes most to the length of the nozzle contour and is used to turn the flow axially. Beyond this section, a uniform axial flow with the desired Mach number is achieved.

The mass flow rate across the characteristic surface remains constant throughout the nozzle [6]. In this paper, the entire nozzle contour associated with the turning section or simply the turning contour is developed on this principle of consistency of mass flow rate. The development of turning contour begins by dividing the final characteristic line 'SL' into 'n+1' nodes (n is user dependent) represented as $(i,j),(i+1,j),\ldots,(i+x,j),\ldots,(i+n,j)$ as shown in Fig. 5.

Property at any node $(i+1,j+y)$ on the first RRC is obtained by using the IPS on a node lying on the same RRC just preceding the above node, i.e., $(i+1,j+y-1)$ and a corresponding node $(i,j+y)$ lying on the last RRC extending from the circular arc extension region.

$$g(i+1,j+y)=\mathrm{IPS}\left[g(i,j+y),g(i+1,j+y-1)\right]. \tag{14}$$

The total mass flow rate through a differential element of length 'ds' across any characteristic line making an inclination angle ϕ with the nozzle axis as shown in Fig. 6 is given as [6]:

$$\dot{m}=\int\frac{\rho w\sin(\phi-\theta)}{\sin\phi}(2\pi y)dy \tag{15}$$

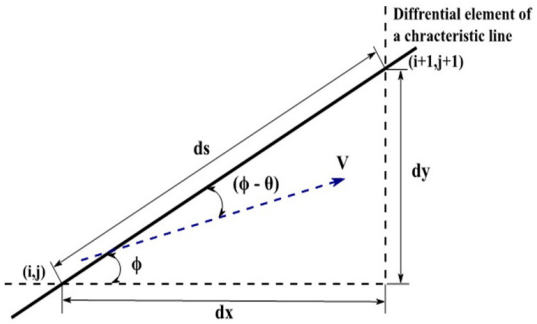

Fig. 6. Mass flow rate through the differential element of the control surface [6].

where ρ, w and θ represent the density, speed, and turning angle taken uniform over that element, and their values are known to us only at the nodes. Therefore, the above integral is written in a discrete summation form.

For a nodal location (i, j) in Fig. 6,

$$k(i,j)=\frac{\rho(i,j)\,w(i,j)\sin\left[\tan^{-1}\left\{\frac{\Delta y(i,j)}{\Delta x(i,j)}\right\}-\tan^{-1}\left\{\frac{v(i,j)}{u(i,j)}\right\}\right]y(i,j)}{\sin\left[\tan^{-1}\left\{\frac{\Delta y(i,j)}{\Delta x(i,j)}\right\}-\tan^{-1}\left\{\frac{v(i,j)}{u(i,j)}\right\}\right]} \quad (16)$$

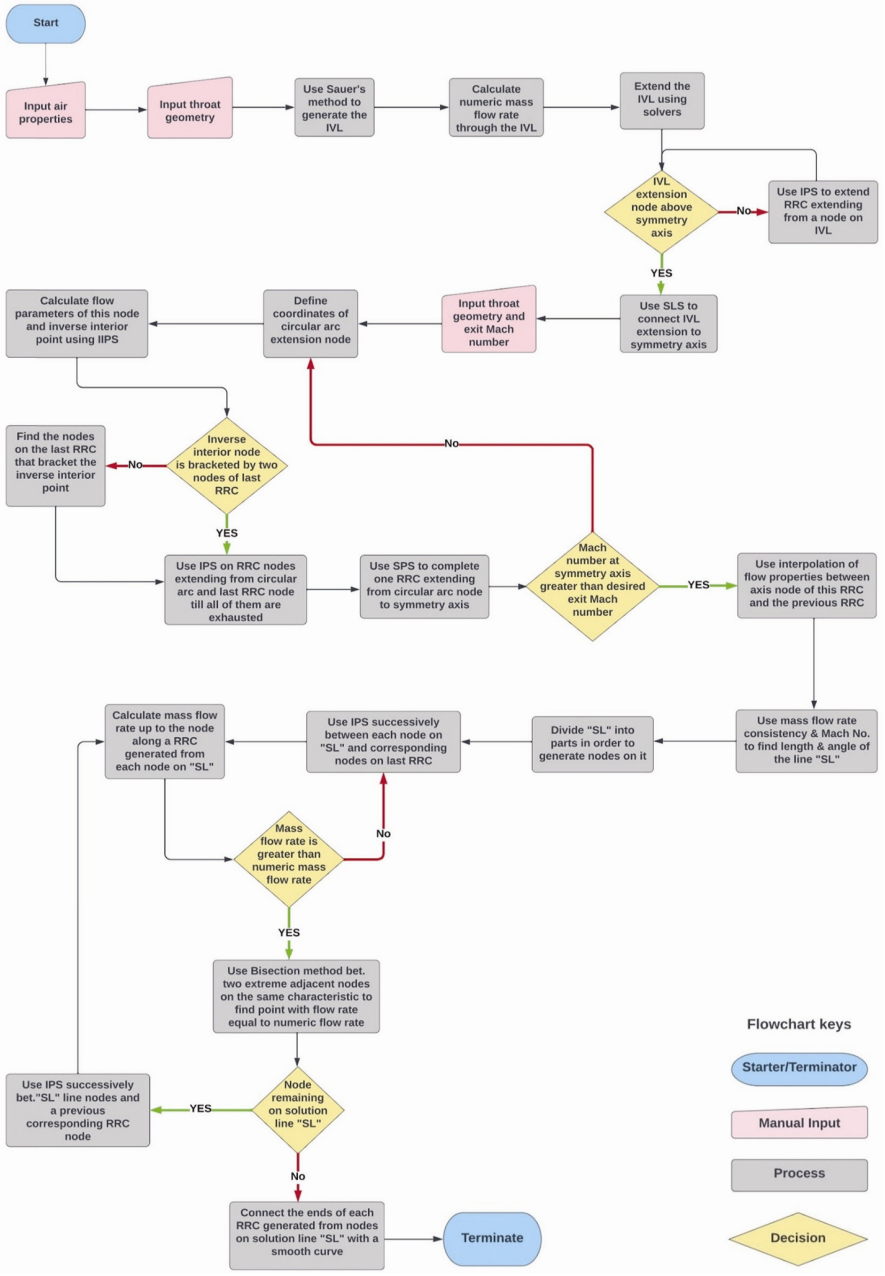

Fig. 7. Flow chart for the design of an Ideal contour nozzle.

where $\Delta y(i,j)=\{y(i+1,j+1)-y(i,j)\}$ and $\Delta x(i,j)=\{x(i+1,j+1)-x(i,j)\}$ and $k(x,y)=\dfrac{\rho w \sin(\phi-\theta)y}{\sin\phi}$.

The mass flow rate through a differential element 'ds' in Fig. 6 is (using the trapezoidal method [26]):

$$\dot{m}=\pi^{*}\left[\{k(i,j)+k(i+1,j+1)\}\{y(i+1,j+1)-y(i,j)\}\right]. \quad (17)$$

The terminal point of the characteristic line (RRC) through which the turning contour would pass is determined by the consistency of mass flow rate and, as such, the first RRC of the turning section shown in Fig. 5 will terminate when

$$\dot{m}(i,j)+\dot{m}(i+1,j)+\dot{m}(i+1,j+1)+\ldots+\dot{m}(i+1,j+y)=\dot{m}_{num}. \quad (18)$$

Limiting the length of the characteristic line according to mass flow rate consistency is done by applying a series of bisection methods between nodes on the same characteristic that bracket the numeric mass flow rate (e.g., P and P' in Fig. 5). A point is located between the bracketing nodes up till the mass flow rate is exactly equal to the numeric mass flow rate.

This terminates one characteristic line, and the entire procedure is continued for all the nodes on 'SL' until the complete profile representing the end of characteristics is obtained. This profile forms the turning section of the Ideal contour nozzle. A brief summary of the various steps employed for the development of ICN is provided through the following flowchart (Fig. 7).

3. Results and discussion

3.1 Developing the Ideal contour nozzle

In the present computational model, boundary layer effects and chemical reactions are neglected throughout the flow field. Stagnation temperature and stagnation pressure of 800 K and 7 MPa, respectively, are used throughout the analysis. A robust MATLAB program for generating the ICN and analyzing the fluid properties is developed. Mesh-fineness is controlled through parameters such as n, $\Delta\theta_c$, and h.

Figs. 8 and 9 are the profiles of two ICNs, one with a downstream radius of curvature (ρ_d) equal to 2 and the other with a longer ρ_d equal to 16. These figures reveal the non-uniform mesh developed by the implementation of solvers for the discretization of the problem domain. Both nozzles were developed from the implementation of the steps provided in the flowchart.

One way to check the accuracy of the present method is to compare the final area ratio of the supersonic nozzle that is obtained by applying the MoC with the one-dimensional area ratio isentropic relationship with the same specific heat and final Mach number [27]. These two solutions should coincide if the flow is assumed to be uniform and the cross-sectional area

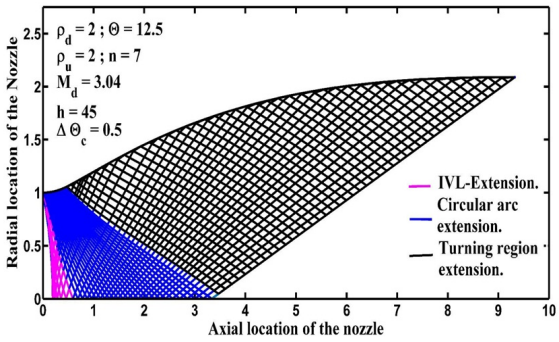

Fig. 8. *ICN* for a downstream radius of curvature, ρ_d = 2.

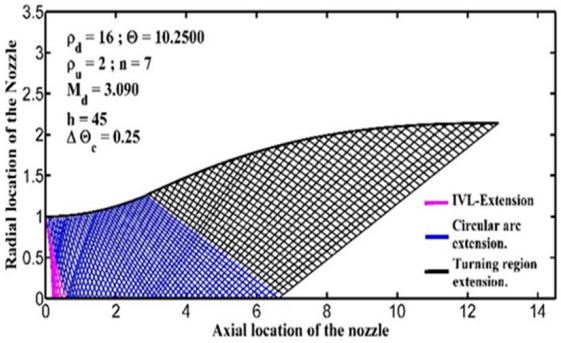

Fig. 9. *ICN* for a downstream radius of curvature, ρ_d = 16.

is assumed to be perpendicular to the flow direction at both the throat and the nozzle exit. In the present case, since a two-dimensional flow is assumed at the nozzle throat, the difference between the solutions generated by MoC and the quasi-one-dimension area-Mach relation would include the numerical error and the effect of two-dimensional flow at the nozzle inlet. Using the MoC, the expansion ratio of the above two nozzles for the aforementioned Mach numbers yielded a difference of 0.6187 and 0.6128 percent, respectively, when compared with the values of quasi-one-dimension area-Mach equations present in various texts [28].

3.2 Discharge coefficient and throat geometry relation

The nozzle discharge coefficient (C_d) is the ratio of numerically calculated mass flow rate ($\dot{m}_{num}$) crossing the nozzle throat section to the mass flow rate that would cross that section if the flow were one-dimensional ($\dot{m}_{(1-D)}$). The numeric mass flow rate is always less than the one-dimensional mass flow rate due to the two-dimensional flow effect in the throat, and this reduction in the mass flow rate can be measured by the values of C_d.

It is evident from Fig. 10 that the calculated curve for the values of discharge coefficient using the present analysis approaches the experimentally determined values of Back [29, 30] when the normalized throat radius of curvature is 2. However, for R_a = 0.625, the resulting curve differs considerably

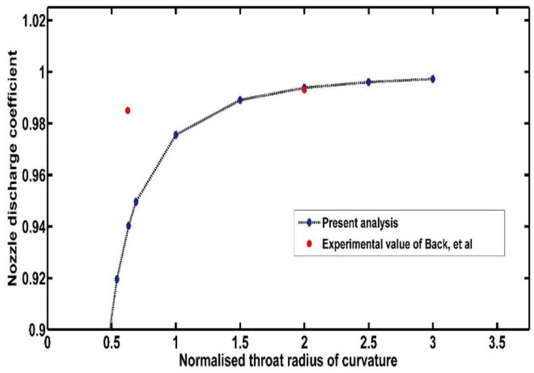

Fig. 10. Variation of the discharge coefficient with R_a.

from the experimental values. Since the scope of the present study is for nozzles having $R_a \geq 2$, it can be employed for studying the transonic region and developing the IVL. As the value of R_a keeps on increasing, the flow coefficient approaches a limiting value of 1, i.e., the flow becomes almost one-dimensional.

3.3 Stability of supersonic flow in the divergent section of ICN

To understand the effect of the input geometric parameters (ρ_u , ρ_d , t_h, etc.) on the stability (in terms of shock) of the supersonic flow inside the divergent section of the ICN, sixteen (16) nozzles with varying geometries were computationally tested and compared. Their input design parameters are provided in Table 1, which contains three groups of nozzles. Each nozzle operates under the same stagnation and ambient conditions and expands the flow to Mach number 3. Group 1 nozzles are used to study the effect of downstream radius of curvature (ρ_d) on the thermodynamic and flow properties of the working fluid in the divergent section. The convergent side geometry is kept fixed with the smallest possible value of the upstream radius of curvature (ρ_u = 2) for a unit throat height (i.e., R_a = 2, resulting from Subsec. 3.2). Group 2 nozzles are used to study the effect of the upstream radius of curvature (ρ_u) of the nozzle on the gas properties as the divergent side geometry is kept fixed, and group 3 nozzles are used to study the variation of gas properties in symmetric nozzles (equal upstream and downstream radius of curvature).

Fig. 11 shows the variation of Mach number along the axis of symmetry (only up to point 'S' in Fig. 4) of group 1 nozzles from Table 1. Along a certain initial length in the divergent section of the nozzle, Mach numbers (and other thermodynamic and flow properties) do not vary with the downstream radius of curvature. This initial Mach number curve is same for all the nozzles (N1-N10) and corresponds to the nodes along the axis that are a part of the IVL extension. The properties in this region depend only on the upstream nozzle geometry (i.e., R_a) and are independent of the downstream profile, as can be observed from Fig. 11. An Instant drop in the Mach number values is observed for high values of ρ_d that corresponds to

Table 1. Design parameters for varying nozzle geometry.

Name	Nozzle number (nomenclature)	Upstream radius of curvature (ρ_u)	Downstream radius of curvature (ρ_d)
Group 1 (M_d = 3.00)	Nozzle 1 (N1).	2.00	20.00
	Nozzle 2 (N2).	2.00	18.00
	Nozzle 3 (N3).	2.00	16.00
	Nozzle 4 (N4).	2.00	14.00
	Nozzle 5 (N5).	2.00	12.00
	Nozzle 6 (N6).	2.00	10.00
	Nozzle 7 (N7).	2.00	2.00
	Nozzle 8 (N8).	2.00	1.00
	Nozzle 9 (N9).	2.00	0.500
	Nozzle 10 (N10).	2.00	0.250
Group 2 (M_d = 3.00)	Nozzle 1 (N1).	2.000	20.00
	Nozzle 11 (N11).	4.000	20.00
	Nozzle 12 (N12).	6.000	20.00
	Nozzle 13 (N13).	20.000	20.00
Group 3 (M_d = 3.00)	Nozzle 7 (N7).	2.000	2.000
	Nozzle 14 (N14)	5.000	5.000
	Nozzle 15 (N15)	10.00	10.00
	Nozzle 16 (N16)	15.00	15.00
	Nozzle 13 (N13)	20.00	20.00

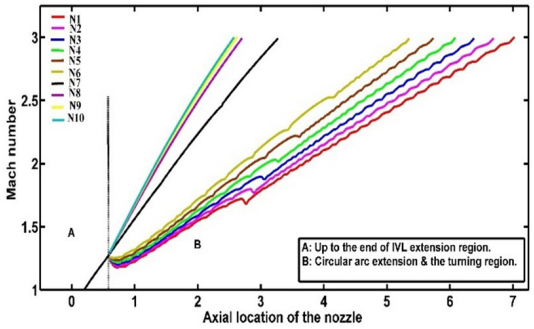

Fig. 11. Mach number variation along the nozzle axis up to point 'S' for group1 nozzles.

the first node on the axis of symmetry resulting from the circular arc boundary immediately downstream of the throat. This instant initial drop in Mach number represents a weak shock[1] and is termed a primary shock, which can also be viewed clearly from Fig. 11.

The location of the primary shock is independent of the downstream radius of curvature (ρ_d) of the nozzle, while its intensity is proportional to the value of the difference between the upstream and downstream radius of curvature of the nozzle (when upstream radii are kept constant and have the minimum possible value for a unit throat height). These weak shocks that may generally be neglected under normal circumstances should be given utmost importance as they predict the possibility of a strong shock for high values of the difference

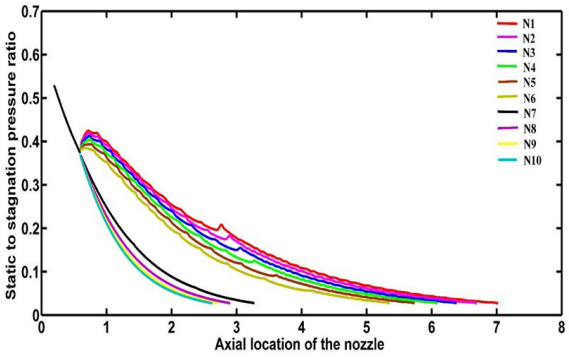

Fig. 12. (P/P_0) variation along the nozzle axis for varying radius ratio (ρ_d/ρ_u).

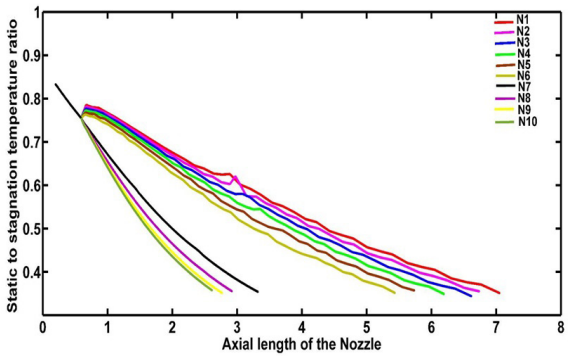

Fig. 13. (T/T_0) variation along the nozzle axis for varying radius ratio (ρ_d/ρ_u).

between the convergent and divergent radius of curvature of an ICN. In some cases, where this difference was very high, the calculations broke down, resulting in complex numbers, due to the formation of subsonic regions. As the difference between the values of upstream and downstream radius of curvature becomes small, a smooth variation of Mach number along the nozzle axis is observed (N7 in Fig. 11). For very small values of ρ_d (i.e., *N*8, *N*9, *N*10), the Mach number curves start to converge without any jump in the property values. Fig. 11 also predicts the formation of a second shock that lies deep within the circular arc extension region for nozzles N1, N2, N3, and N4. As the value of the downstream radius of curvature increases, the intensity of the secondary shock also increases. It moves upstream towards the throat, where it can interact with the primary shock and, as such, may result in a stronger shock. The instant drop in the Mach numbers resulting in the primary and secondary shock should, in turn, elevate the static pressure and static temperature abruptly and this is shown in Figs. 12 and 13, respectively.

The downstream radius of curvature (ρ_d) plays an important role in controlling the velocity gradient of the flow and the length of the divergent section of ICN. Fig. 14 shows the effect of ρ_d on the length and nature of flow in the nozzle divergent section by plotting contours of nozzles from group 1 along with a constant iso-Mach curve (M_{iso} = 1.500) within these nozzles.

With the increase in ρ_d , the iso-Mach line shifts deeper into the divergent section of the nozzle, indicating a decrease in the

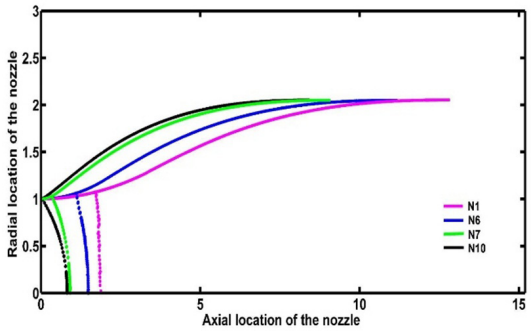

Fig. 14. Variation of nozzle contour and iso-Mach (M_{iso} = 1.50) line with ρ_d.

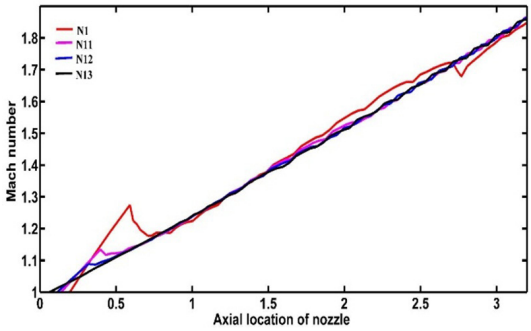

Fig. 15. Mach number variation along the nozzle axis for group 2 nozzles.

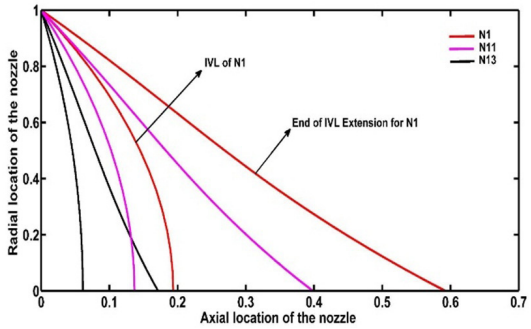

Fig. 16. Effect of ρ_u on the axial length of IVL extension along the axis of symmetry.

velocity gradient and a corresponding increase in the length of the nozzle in order to achieve the desired Mach number (M_d = 3.00). The curvature of the iso-Mach lines also reduces, indicating the effect of the downstream radius of curvature in producing a dominant one-dimensional flow.

Fig. 15 shows the variation of Mach number along the axis of symmetry (within a region of interest in the circular arc extension region) of group 2 nozzles from Table 1. Unlike group 1 nozzles, the Mach numbers, and other properties, are no longer constant for a certain initial length along the axis of symmetry in the group 2 nozzles. The contribution, in terms of length, of the IVL extension along the axis of symmetry increases with a decrease in the upstream radius of curvature (ρ_u) as shown in Fig. 16 and numerically validated by the data provided in Table 2. So, as the value of ρ_u decreases, an

Table 2. Length of the IVL extension along the axis of symmetry for group 2 nozzles.

Nozzle nomenclature	ρ_u	ρ_d	X_s	X_{end}	$X_{end} - X_s$
Nozzle 1 (N1)	2.000	20.00	0.1936	0.5926	0.3990
Nozzle 11 (N11)	4.000	20.00	0.1369	0.3983	0.2614
Nozzle 12 (N12)	6.000	20.00	0.1118	0.3200	0.2082
Nozzle 13 (N13)	20.000	20.00	0.06124	0.1715	0.1102

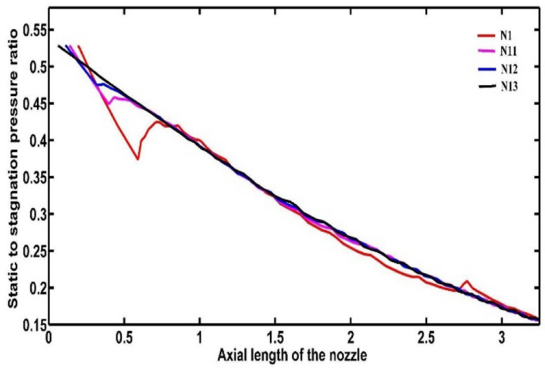

Fig. 17. (P/P_0) variation along the nozzle axis for group 2 nozzles.

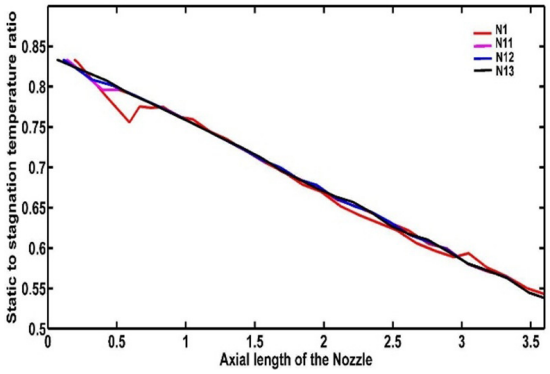

Fig. 18. (T/T_0) variation along the nozzle axis for group 2 nozzles.

increase in both the IVL extension region and property (i.e., Mach number) gradients is observed in the flow field immediately downstream of the throat (along the nozzle axis). This region is independent of the downstream radius of curvature.

Nozzle N1 has the maximum shock intensity among the group 2 nozzles, and as the value of ρ_u increases for a fixed ρ_d, shock intensity decreases rapidly, and the shock moves closer to the throat. A secondary shock is observed for nozzle (N1), but gets eliminated immediately as the value of ρ_u increases. The drop in the Mach numbers along the nozzle axis should be accompanied by an abrupt rise in static pressures and static temperature as shown in Figs. 17 and 18, respectively.

N7 and N13 nozzles stand out among the rest of the members from group 1 and group 2 nozzles in having the smoothest variation in Mach number along the nozzle axis. Both these

Table 3. Effect of exit Mach number on the circular arc extension region and length of the nozzle.

M_d	L_{nozzle}	θ_{exp}	A_{ratio}
1.7560	2.9882	3.9000	1.3845
2.0000	3.8920	5.8999	1.6757
2.2490	4.9427	7.7999	2.0824
2.4970	6.1302	9.4999	2.6148
2.7530	7.5356	11.0999	3.3267
2.9930	9.0550	12.4999	4.1800
3.2429	10.8696	13.7999	5.3005
3.5097	13.0717	14.9999	6.8088

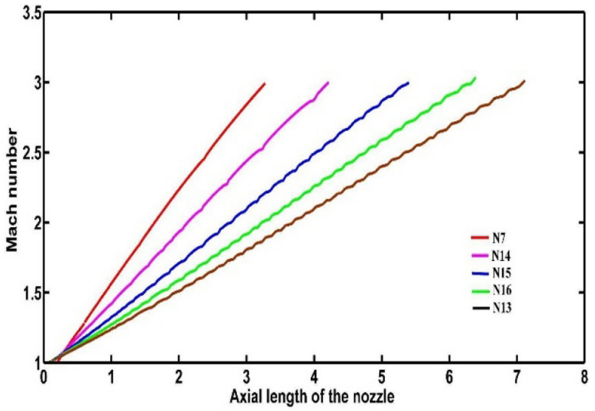

Fig. 19. Mach number variation along the nozzle axis (up to point 'S' in Fig. 4) for group 3 nozzles.

nozzles are symmetric nozzles. This observation is supported further by analyzing variation in Mach numbers along the nozzle axis in only symmetric nozzles or the group 3 nozzles (Fig. 19).

Smooth variation in Mach numbers and other thermodynamic properties is observed in group 3 nozzles and, as such, they form the best choice for selecting an ICN. The variation in Mach numbers along the nozzle axis for various nozzles in group 3 is almost linear with small perturbations. Reducing the radius of curvature of the symmetric nozzles increases the gradient of the Mach number curve along the nozzle axis, which in turn reduces the length of the circular arc extension region required to expand the flow to a desired exit Mach number resulting in an overall shorter nozzle.

It is also observed that a change in the desired exit Mach number (M_d) for a nozzle with fixed input geometry, stagnation, and ambient conditions has no effect on the location or intensity of either of the shocks. A higher (or lower) desired Mach number (M_d) would result in a longer (or shorter) circular arc extension region and a corresponding longer (or shorter) nozzle. This region controls the expansion of the flow to achieve a desired Mach number. This observation is validated by the data in Table 3 shown above (fixed input geometric parameters: (t_h = 1, $\rho_u = \rho_d$ = 2* t_h , $\Delta\theta_c$ = 0.1)).

4. Conclusions

An algorithm for developing the perfect or ideal contour nozzle by employing the MoC was discussed, and the effect of the geometric parameters such as the upstream radius of curvature (ρ_u) and downstream radius of curvature (ρ_d) on the stability of the supersonic flow field in the divergent section of the nozzle was studied. Sixteen ICNs with different nozzle geometries were analyzed, and the following conclusions are drawn:

1) The throat geometry of the nozzle has a significant effect on the stability of the flow inside the divergent section of the ICN. An abrupt reduction in Mach number (weak shocks) can be observed along the nozzle axis when the difference between the radius of curvature on the convergent and divergent sides is large. The intensity of this shock enhances with the increase in the downstream radius of curvature while the upstream radius of curvature is kept fixed and has a small value (ρ_u = 2). The location of the initial shock, which is formed immediately downstream of the nozzle throat (termed the primary shock), depends on the normalized throat radius of curvature (R_a). The upstream nozzle geometry plays a very important role in reducing the intensity of primary shock and controlling its location when the downstream radius of curvature is kept high and fixed (ρ_d = 20). Thus, weak shocks are formed even in ICN when the radius of curvature upstream and downstream of the throat is highly asymmetric, and the intensity of this weak shock is a function of both the radii of curvature.

2) There exists a region, however small, within the divergent section of the perfect nozzle in which the thermodynamic and flow properties of the working fluid are independent of the wall profile of the divergent section. This region lies immediately downstream of the throat, and the properties of the fluid inside this region are defined by the upstream throat geometry (i.e., ρ_u *and* t_h). The smaller the value of ρ_u (for a unit t_h), the higher is the extension of this region, in terms of volume. The axial length of this region decreases as one moves radially from the axis of symmetry to the nozzle wall.

3) Group 3 or symmetric nozzles ($\rho_u = \rho_d$) produced the best results in terms of flow stability. The thermodynamic and flow properties of the supersonic flow vary smoothly along the axis of symmetry in the divergent section of the symmetric nozzles. With a reduction in the radius of curvature in these nozzles, the gradient of the Mach number along the nozzle axis increases. As such, a shorter symmetric nozzle would be required to expand the flow to a desired exit Mach number without the formation of shocks. Thus, among all the ICNs tested, symmetric nozzles stand out in developing supersonic flow with smooth property variations. Within these nozzles, the one with the minimum radius of curvature would have the minimum length and the lowest corresponding weight.

Nomenclature

MoC : Method of characteristics
ICN : Ideal contour nozzle
MATLAB : Matrix laboratories
LRC : Left running characteristic
RRC : Right running characteristic
IPS : Internal point solver
SPS : Symmetry point solver
IIPS : Inverse interior point solver
IVL : Initial value line
M_{iso} : Iso-Mach
TIC : Truncated ideal contour
γ : Ratio of specific heats
R_a : Normalised throat radius of curvature
ρ_d , ρ_u : Downstream and upstream radius of curvature
θ_{in} : Entrance angle
u,v : Axial and radial velocity components
x,y : Axial and radial coordinates
δ : 0, 1 for a planar flow and axis-symmetric flow, respectively
V : Velocity vector in the flow field
a : Acoustic speed of sound
M : Mach number
t_h : Throat height
w : Flow velocity (scalar)
θ : Angle between flow direction and nozzle axis
ϕ : Angle between the characteristic line and nozzle axis
R : Specific gas constant
s : Length of a characteristic line
$\dot{m}$: Mass flow rate
ζ : Coefficient of linear axial velocity perturbation
$\Delta\theta_c$: Angular increment of the downstream circular arc
$\dot{m}_{num}$: Numeric mass flow rate
$(\dot{m}_{(1\text{-}D)})$: One-dimensional mass flow rate
n : Number of points taken on IVL
M_d : Desired exit Mach number
α : Angle between streamline tangent and tangent to characteristic lines
h : Number of nodes taken on the last LRC
β : Angle between the nozzle axis and the final LRC
g : Thermodynamic and flow properties of the fluid as a function of the location
P_0, P : Stagnation and static pressure
T_o, T : Stagnation and static temperature
ρ_o, ρ : Stagnation and static density
C_d : Discharge coefficient
X_s : First node of IVL on the axis of symmetry
X_{end} : Last node of IVL extension on the axis of symmetry
L_{nozzle} : Length of the nozzle
θ_{exp} : Downstream circular arc expansion angle
A_{ratio} : Area ratio

References

[1] L. C. Squire, *Modern Compressible Flow: With Historical Perspective*, Second Edition, McGraw-Hill Book Co., Berks (1991) 248-248.

[2] R. J. Hartfield and J. E. Burkhalter, A complete and robust approach to the axisymmetric method of characteristics for nozzle design, *51st AIAA/SAE/ASEE Joint Propulsion Conference*, Orlando (2015).
[3] A. H. Shapiro and G. M. Edelman, Method of characteristics for two-dimensional supersonic flow—graphical and numerical procedures, *J. Appl. Mech.* (1947) A154-A162.
[4] E. C. Guentert and H. E. Neumann, *Design of Axisymmetric Exhaust Nozzles by Method of Characteristics Incorporating a Variable Isentropic Exponent*, Technical Report R-33, National Aeronautics and Space Administration (1959).
[5] C. G. Guderley and E. Hantsch, Beste formen für achsensymmetrische überschall schubdüsen, *Zeitschrift für Flugwissenschaften*, 3 (9) (1955) 305-313.
[6] G. V. R. Rao, Exhaust nozzle contour for optimum thrust, *J. of Jet Propulsion*, 28 (6) (1958) 377-382.
[7] J. H. Ahlberg et al., Truncated perfect nozzles in optimum nozzle design, *ARS Journal,* 31 (5) (1961) 614-620.
[8] L. V. Gogish, *Investigation of Short Supersonic Nozzles (Issledovanie Korotkikh Sverkhzvukovykh Sopel)*, Foreign Technology Div Wright-Patterson AFB Ohio (1967).
[9] R. Sauer, *General Characteristics of the Flow through Nozzles at Near Critical Speeds*, Technical Memorandum No. 1147, National Advisory Committee for Aeronautics (1947).
[10] I. M. Hall, Transonic flow in two-dimensional and axially symmetric nozzles, *The Quarterly J. of Mechanics and Applied Mathematics,* 15 (4) (1962) 487-508.
[11] J. R. Kliegel and J. N. Levine, Transonic flow in small throat radius of curvature nozzles, *AIAA J.,* 7 (7) (1969) 1375-1378.
[12] A. Haddad and H. Kbab, Application of de-laval nozzle transonic flow field computation approaches, *International J. of Mechanical, Aerospace, Industrial, Mechatronic and Manufacturing Engineering,* 7 (2) (2013) 1093-1098.
[13] T. Zebbiche and Z. Youbi, Effect of the stagnation temperature on supersonic flow parameters application for air in nozzles, *J. of Engineering Thermophysics,* 16 (2) (2007) 53-62.
[14] M. Salhi, T. Zebbiche and A. Mehalem, Stagnation pressure effect on the supersonic flow parameters with application for air in nozzles, *The Aeronautical J.,* 120 (1224) (2016) 313.
[15] J. D. Hoffman, Design of compressed truncated perfect nozzles, *J. of Propulsion and Power,* 3 (2) (1987) 150-156.
[16] K. Davis et al., Experimental and computational investigation of a dual-bell nozzle, *53rd AIAA Aerospace Sciences Meeting*, Kissimmee (2015).
[17] M. J. Zucrow and J. D. Hoffman, *Gas Dynamics. Volume 2-Multidimensional Flow,* John Wiley and Sons, New York (1977).
[18] J. Maurice, *Gas Dynamics*, John Wiley and Sons, New York (1976).
[19] B. Carnahan, H. A. Lither and J. O. Wilkes, *Applied Numerical Methods*, John Wiley and Sons, New York (1969).
[20] S. D. Conte and C. de Boor, *Elementary Numerical Analysis: An Algorithmic Approach*, Society for Industrial and Applied Mathematics, Philadelphia (2017).
[21] J. D. Hoffman, Accuracy studies of the numerical method of characteristics for axisymmetric, steady supersonic flows, *J. of Computational Physics*, 11 (2) (1973) 210-239.
[22] A. Hadjadj and M. Onofri, Nozzle flow separation, *Shock Waves*, 19 (3) (2009) 163-169.
[23] L. Nave and G. Coffey, Sea level side loads in high-area-ratio rocket engines, *9th Propulsion Conference*, Las Vegas (1973).
[24] J. D. Anderson, *Modern Compressible Flow*, McGraw-Hill Education, New York (2003).
[25] J. D. Hoffman, *A Computer Program for the Performance Analysis of Scarfed Nozzles*, Battelle Columbus Labs Research Triangle Park NC (1984).
[26] P. K. Henrici, *Elements of Numerical Analysis,* Wiley, New York (1964).
[27] Y. Nachshon, Simple and accurate calculation of supersonic nozzle contour, *AIAA J.,* 21 (5) (1983) 783-784.
[28] H. W. Liepmann and A. Roshko, *Elements of Gas Dynamics*, Courier Corporation (2001).
[29] L. H. Back, P. F. Massier and H. L. Grier, Comparison of measured and predicted flows through conical supersonic nozzles, with emphasis on the transonic region, *J. of the American Institute of Aeronautics and Astronautics*, 3 (9) (1965) 1606-1614.
[30] R. F. Cuffel, L. H. Back and P. F. Massier, The transonic flowfield in a supersonic nozzle with small throat radius of curvature, *J. of the American Institute of Aeronautics and Astronautics*, 7 (7) (1969) 1364-1366.

Khalid Rafiq is an Engineer at Tata Advanced Systems Limited. He received his B.Tech. in Mechanical Engineering from the Institute of Technology, University of Kashmir. His research interests are computational mechanics and data-driven techniques.

Mumin Rasheed received his B.Tech. in Mechanical Engineering from the Institute of Technology, University of Kashmir. His research interests are engineering fluid mechanics, CFD, aero-thermodynamics, and compressible fluid flow.

Mir Moin Afzal received his B.Tech. in Mechanical Engineering from the Institute of Technology, University of Kashmir. His research interests are AI, robotics, compressible fluid flow, CFD, and aerodynamics.

Junaid H Masoodi is an Assistant Professor of Mechanical Engineering, Institute of Technology, University of Kashmir. He received his Ph.D. in Mechanical Engineering from the National Institute of Technology, Srinagar. His research interests include CFD analysis of turbomachinery, compressible fluid flow, erosive wear, fracture & fatigue.